Conjugated Polyelectrolytes: Conformation-Sensitive Optical Probes for Detection of Amyloid Fibril Formation†

K. Peter R. Nilsson,*,‡ Anna Herland,‡ Per Hammarström,§ and Olle Inganäs‡

Biomolecular and Organic Electronics, and Chemistry, Departments of Physics and Measurement Technology, Biology, and Chemistry, Linköpings University, SE-581 83 Linköping, Sweden

Received December 10, 2004; Revised Manuscript Received January 6, 2005

ABSTRACT: The in vivo deposition of amyloid fibrils is a hallmark of many devastating diseases known as the amyloidoses. Amyloid formation in vitro may also complicate production of proteins in the biotechnology industry. Simple, sensitive, and versatile tools that detect the fibrillar conformation of amyloidogenic proteins are thus of great importance. We have developed a negatively charged conjugated polyelectrolyte that displays different characteristic optical changes, detected visually or by absorption and emission, depending on whether the protein with which it forms a complex is in its native state or amyloid fibril conformation. This simple, rapid, and novel methodology was applied here to two amyloidogenic proteins, insulin and lysozyme, and its validity for detection of their fibrillar conformation was verified by currently used methods such as circular dichroism, transmission electron microscopy, and Congo red absorption.

The development of materials capable of detecting changes in biological samples is of great interest, due to their potential for being used as analytic tools. In this regard, conjugated polyelectrolytes (CPs)[1] have been used to detect biospecific interactions through their impact on the conditions for photoinduced charge or excitation transfer (*1*−*6*) and through the conformational alterations of the polyelectrolyte chains (*7*−*9*). Recent studies (*10*−*12*) have also shown that CPs can be used as novel optical tools for the detection of conformational changes of biomolecules. The conformational flexibility of polymers, also found in conjugated polyelectrolytes, allows direct connection between the geometry of chains and the resulting electronic structure and processes. This does not necessarily require charge transfer, but requires that the conjugated polyelectrolyte chain geometry will be governed by biomolecules. Hence, it would be of great interest to use dominant biomolecules, forcing the geometry of the conjugated polyelectrolytes. If conformational changes of biomolecules could lead to different conformations of the polyelectrolyte backbone, an alteration of the absorption and emission properties from the polyelectrolyte would be observed.

Natural biopolymers, such as proteins, frequently alter their conformations due to different external stimuli. The importance of conformational changes of proteins leading to pathogenic states, such as Alzheimer's disease, the systemic amyloidosis, and transmissible spongiform encephalopathy, has been well documented (*13*−*16*). Especially under conditions that destabilize the native state, proteins can aggregate into characteristic fibrillar assemblies, known as amyloid fibrils (*17*−*19*). Insulin (Figure 1), a 51-residue polypeptide hormone, has a mainly helical native structure, with its two polypeptide chains linked by one intrachain and two interchain disulfide bonds (*20*, *21*). In vitro, insulin is readily converted to an inactive β-sheet-rich amyloid fibrillar form by incubation at high insulin concentration, acidic pH, and elevated temperatures (*22*, *23*). Nielsen et al. (*24*) have proposed a model for the formation of amyloid fibrils of insulin that starts with hexamer−tetramer−dimer units of the protein in solution. The level of association of the protein depends on factors such as the concentration, pH, and the temperature of the solution. To form fibrils, the hexamer−trimer−dimer units have to dissociate to form the monomeric protein (*25*−*27*). The monomeric units then need to partially unfold and aggregate to produce the nucleus from which amyloid fibrils can grow.

The kinetics of the amyloid fibrillogenesis in vitro by insulin has been studied via many different techniques (*25*−*27*). Conventionally, the presence of amyloid deposits and/or fibrils is studied by staining with small molecule dyes, such as Congo red and thioflavin T (*28*). In this Article, we report a novel conformation-sensitive optical method for the detection of formation of amyloid fibrils in bovine insulin (BI) and chicken lysozyme (CL) based on conformational changes of an anionic polythiophene derivative (Figure 1). A novel optical method for the detection of amyloid fibril formation of insulin is of great importance with respect to the long-term stability of insulin in commercial pharmaceutical formulations used for the treatment of diabetes.

† This work was partially funded by VINNOVA (A.H.) and CENANO, Linköping University. Support from the Swedish foundation for strategic research (SSF) (P.H.), the Wenner-Gren foundations (P.H.), and the Swedish research council (P.H.) is greatly appreciated.

* To whom correspondence should be addressed. Telephone: +46-13-28-17-04. Fax: +46-13-28-89-69. E-mail: petni@ifm.liu.se.

‡ Biomolecular and Organic Electronics.

§ Chemistry.

[1] Abbreviations: CP, conjugated polyelectrolyte; PTAA, poly(thiophene acetic acid); BI, bovine insulin; nBI, native bovine insulin; fBI, BI in amyloid fibrillar form; CL, chicken lysozyme; nCL, native chicken lysozyme; fCL, CL in amyloid fibrillar form.

10.1021/bi047402u CCC: $30.25
Published on Web 02/10/2005

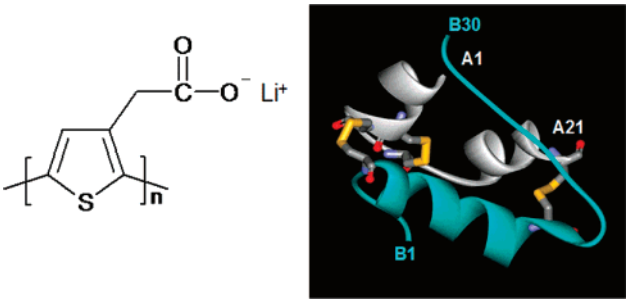

FIGURE 1: Chemical structure of the repeating unit of poly(thiophene acetic acid) (PTAA-Li) (left). Structure of the insulin monomer (right) (PDB entry 1APH) (*21*).

EXPERIMENTAL PROCEDURES

Polymer Synthesis and Preparation of Proteins. The synthesis of the PTAA-Li (Figure 1) was reported elsewhere (*29*). Bovine insulin and hen egg white lysozyme were obtained in pure form from Sigma, and purity was assessed through SDS-PAGE. Absorbance at 280 nm was employed for concentration determinations using $\epsilon 280 = 5840\ M^{-1}\ cm^{-1}$ and $\epsilon 280 = 37\,750\ M^{-1}\ cm^{-1}$ for insulin and lysozyme, respectively. Insulin was dissolved in 2 M guanidine hydrochloride, dialyzed versus three changes of 25 mM HCl at +4 °C, and stored (0.5−2.0 mM) at +4 °C, where the solutions were stable for several weeks. Lyophilized lysozyme from hen egg white, obtained from Sigma, was dissolved in dH_2O to a concentration of 0.7 mM. The protein was dialyzed either as above or against 10 mM Na-phosphate buffer, pH 7.5. Filtered (0.45 μm) stock solutions were made to 0.5 mM. Collagen type I (from white rabbit skin; Sigma) was dissolved in 0.5 M HAc to a final concentration of 320 μM.

Amyloid Fibril Formation. A stock solution containing 320 μM bovine insulin in 25 mM HCl was prepared. The solution was placed in a water bath kept at 65 °C to induce amyloid formation. Samples were taken and analyzed during a time period of 3 days. Lysozyme fibrils were made through incubation of the protein in 25 mM HCl at 65 °C for 700 h.

Microscopy Experiments. Aliquots collected at different time points during fibril formation were diluted in 25 mM HCl and applied to carbon-coated grids for 2 min. The grids were washed and negatively stained with uranyl acetate 2% (wt/vol) in water and air-dried before being examined in a Phillips EM400 transmission electron microscope (TEM) at an accelerating voltage of 120 kV.

Atomic force microscopy (AFM) imaging was preformed by standard procedures in tapping mode on a SFM-Nanoscope III, Digital Instruments, with a J scanner. Cantilevers for tapping mode were obtained from NT-MDT. For the AFM observations, 10 μL of 1.0 mg mL^{-1} PTAA-Li in deionized water solution was mixed with 25 mL of the bovine insulin solution (320 mM in 25 mM HCl incubated in 65 °C for 10 h) and diluted 10 times with a stock buffer solution (Na-phosphate pH 7.0). The sample was incubated for 5 min at room temperature. A drop was applied to a hydrophobic silicon (100) surface with a monolayer of DDS (dichlorodimethylsilane), incubated for 2 min, and excess protein was removed by extensive rinsing in deionized water. The fluorescence from the PTAA/bovine insulin complexes on the hydrophobic silicon substrate was recorded with an epifluorescence microscope (Zeiss Axiovert inverted microscope A200 Mot) equipped with a CCD camera (Axiocam HR), using a 470/40 nm filter (LP515, exposure time: 1500 ms). For observation of birefringence complexes of PTAA/bovine insulin prepared as above, the stock buffer solution diluted by 2 times (Na-phosphate pH 7.0) was deposited on glass. An Olympus BH-2 polarization microscope with crossed polarizers was used in transmission mode and with a filter setup to observe the polarization of the emitted light.

Collagen type I (from white rabbit skin; Sigma) was dissolved in 0.5 M HAc to a final concentration of 320 μM. Next, 20 μL of this solution was mixed with 2 μL of the fBI solution (prepared as above) and diluted to a final volume of 100 μL with deionized water. A droplet, 2 μL, of the mixture was place on a microscope slide, and, after drying, the spot was stained with a droplet (1 μL) of the PTAA solution (1.0 mg mL^{-1}) for 1 min. The excess of unbound PTAA was removed by extensive rinsing in deionized water. The fluorescence from the PTAA/protein complexes on the microscope slide was recorded with an epifluorescence microscope (Zeiss Axiovert inverted microscope A200 Mot) equipped with a CCD camera (Axiocam HR), using a 405/30 nm filter (LP450, exposure time: 1500 ms).

Optical Measurements. A stock solution containing 1.0 mg mL^{-1} PTAA-Li in deionized water was prepared. An aliquot, 10 μL, of the polymer solution was mixed with 25 μL of the bovine insulin solution, 15 μL of the lysozyme solution (both at 25 mM in HCl), or 25 μL of the collagen solution (in HAc), and then diluted with a stock Na-phosphate buffer pH 7.0 to a final volume of 1500 μL containing 20 mM Na-phosphate and 5 μM of each protein, respectively. The sample was incubated for 5 min at room temperature, and the emission spectra were recorded with an ISA Jobin-Yvon spex FluoroMax-2 apparatus. All of the spectra were recorded with excitation at 400 nm. A Perkin-Elmer Lambda 9 UV/vis/NIR spectrophotometer was used for the absorption measurements, and the circular dichroism spectra were recorded with an I.S.A. Jobin-Yvon CD6 (5 mm quartz cell). To provide a Congo-red binding assay according to Klunk et al. (*30*, *31*), a solution of 5 μM Congo red (in 20 mM Na-phosphate, 150 mM NaCl, pH 7.0) was incubated with 25 μL of the bovine insulin solution for 5 min at room temperature before the total absorbance of the mixture was measured at 477 and 540 nm. The amount of Congo red bound was used to determine the quantity of fibrils in the solution, according to: mol of Congo red bound/L of amyloid suspension = $(A_{540\ nm}/25\,295) - (A_{477\ nm}/46\,306)$.

RESULTS

Microscopy Measurements and Circular Dichroism Measurements of BI. As previously reported (*22*, *23*), bovine insulin forms amyloid fibrils when incubated in an acidic environment and at elevated temperatures. Temperature-induced fibril formation by BI at 65 °C (320 μM, 25 mM HCl) was followed by CD over a period of 10 h (Figure 2b). After 10 h of incubation of the protein, BI has changed its structure from an α-helical structure to a more β-sheet-rich structure indicative for formation of amyloid fibrils (for details, see Supporting Information). The electron micrographs of BI during the heat incubation show that the conversion from an α-helical structure to a more β-rich

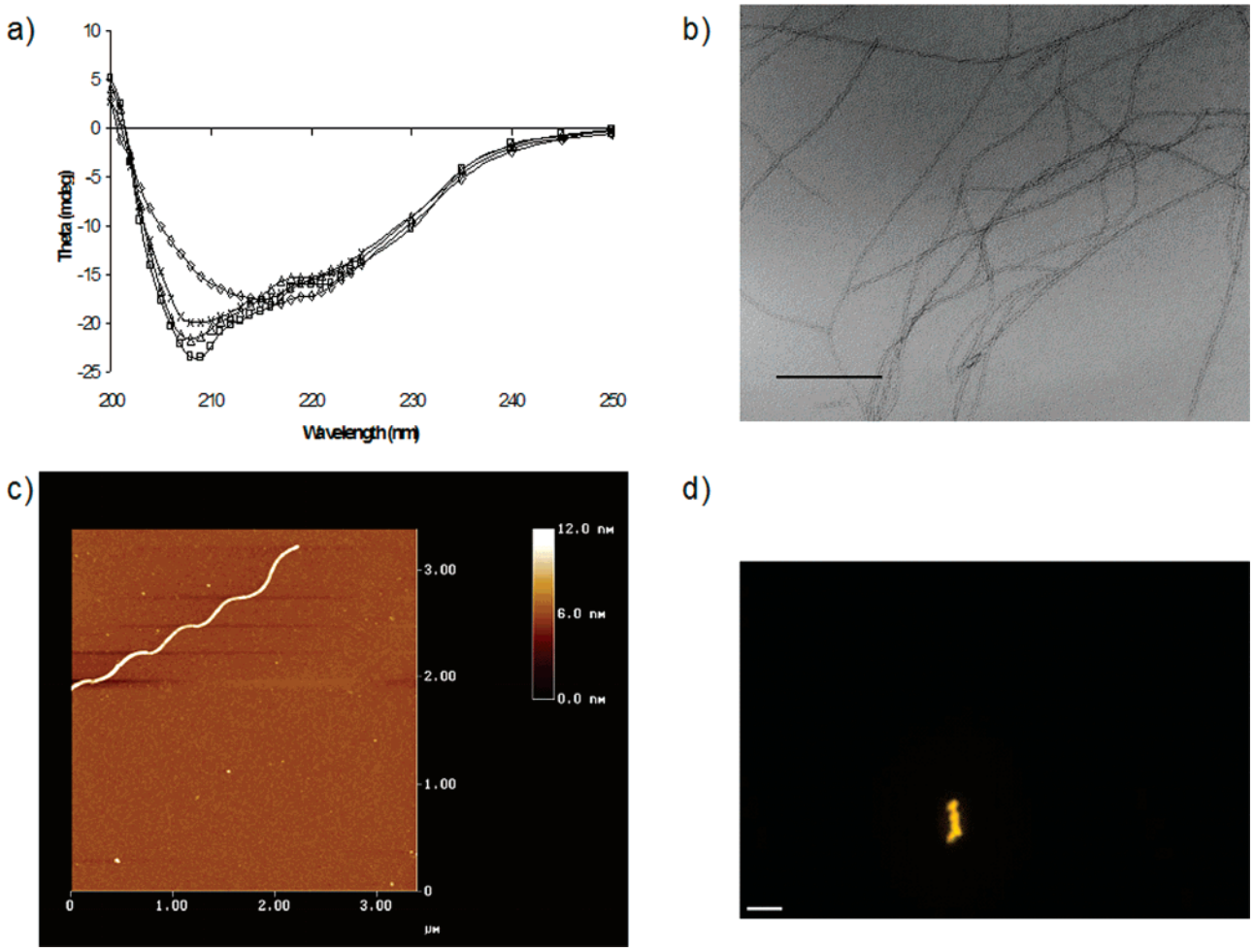

FIGURE 2: (a) Circular dichroism of 5.0 μM bovine insulin in 25 mM HCl solution incubated at 65 °C for 0 h (□), 4 h (△), 6 h (×), and 10 h (◇). (b) Negative staining transmission electron micrograph (top right) of bovine insulin fibrils in 25 mM HCl solution incubated at 65 °C for 10 h. The scale bar represents 200 nm. (c) AFM picture of a single bovine insulin/PTAA fibril. (d) Fluorescence image of the bovine insulin/PTAA fibril complex. The scale bar represents 5 μm. The fibrillation occurred at pH 1.6 and at 65 °C for 10 h. An aliquot was withdrawn, and, after addition of PTAA, the samples were diluted with 20 mM Na-phosphate to pH 7.0 (23 °C) prior to the AFM and fluorescence measurements.

structure is a consequence of the formation of amyloid fibrils (Figure 2b). Prior to heat treatment, no larger aggregates of protein can be seen. During the first 4 h of heat treatment, a large increase in spherical aggregates can be seen over time, and after 4 h a small number of more well-defined fibrils emerge. In the period 4−10 h, a network of fibrils appears followed by a decrease in the amount of spherical aggregates. After 10 h, both smooth fibrils with curvature, indicative of flexibility, and more mature twisted fibrils with an average width of 7−10 nm can be seen (Figure 2b). AFM and fluorescence microscope images of the same hydrophobic Si surface with deposited insulin fibrils also confirm that fibril formation has occurred after 10 h. The AFM image (Figure 2c) shows a large >5 μm long mature amyloid fibril deposited on the silicon surface. The height of the fibril was determined using AFM and was found to be approximately 7 nm. The fluorescence image (Figure 2d) also shows a visible single fibril in complex with PTAA, demonstrating the possibility of using PTAA for optical microscopy staining of such large fibrils. Polarization microscopy reveals the sample to be birefringent (blue-green) in transmitted light and also to emit polarized light in luminescence.

Absorption Measurements of BI and PTAA. The absorption spectra of PTTA-Li (80 μM on a monomer basis) after 10 min incubation in a buffer solution (20 mM Na-phosphate pH 7.0) are shown in Figure 3. An absorption maximum of 446 nm is related to a certain degree of planarization of the polyelectrolyte backbone, suggesting that the buffer solution

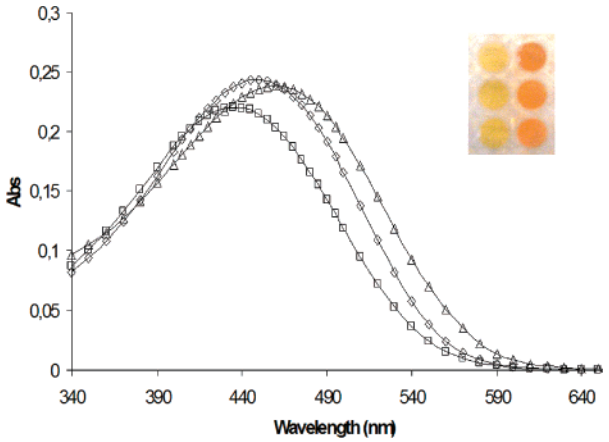

FIGURE 3: Absorption spectra of 80 μM PTAA-Li (on a monomer basis) in 20 mM Na-phosphate pH 7.0 (◇), 20 mM Na-phosphate pH 7.0 with 5.0 μM nBI (□), and 20 mM Na-phosphate pH 7.0 with 5.0 μM fBI (△). The inset shows the microtiter plate wells containing PTAA/nBI (left) and PTAA/fBI (right).

will induce a planarization of the polyelectrolyte backbone. These results are in agreement with earlier studies (*11*, *32*), which suggest that the conformation of the polyelectrolyte in neutral buffer solution is most likely due to electrostatic repulsion forces that act between the carboxylate groups, forcing the polyelectrolyte chains to stretch.

Upon addition of 5 μM native bovine insulin (nBI), the absorption maximum is blue-shifted to 434 nm (Figure 3). This shift is associated with a decrease of the effective conjugation length of the polyelectrolyte backbone, demonstrating that the interaction between PTAA and nBI will force the polyelectrolyte backbone to adopt a more nonplanar conformation. We suggest that the negatively charged carboxyl groups of the polyelectrolyte side chains will most likely interact electrostatically with the positively charged side chains of nBI (1 Arg, 1 Lys, and 2 His). Other amino acids and the peptide backbone are subsequently able to form hydrogen bonds with the carboxyl oxygen of the PTAA side chains, and the polyelectrolyte/protein complex is most likely stabilized by hydrophobic interactions between the thiophene backbone and apolar amino acids of the protein molecule. These interactions will force the polyelectrolyte backbone to adopt a nonplanar conformation and cause a blue shift. A similar blue shift has been observed for PTAA in deionized water and in assemblies with a positively charged peptide where a supramolecular α-helical structure is formed (*11*).

Upon addition of 5 μM (monomer concentration) BI in amyloid fibrillar form (fBI), the absorption maximum is red shifted to 463 nm. This result strongly suggests that binding of PTAA to amyloid fibrils of BI will force the polyelectrolyte backbone to adopt a more rod-shaped conformation. The planarization of the polymer backbone might be a result of the change in the secondary structure of the BI, as the polyelectrolyte will most likely interact differently with the α-helical nBI molecule and the fBI molecule that contains more β-sheet structure. Hence, the alteration of the optical properties from the conjugated polyelectrolyte should be due to a change in the secondary structure of the protein molecule. Interestingly, the shift in absorption for the two different solutions is clearly visible for the human eye. The PTAA/nBI solution is yellow, and the PTAA/fBI solution is orange (Figure 3). This phenomenon is potentially useful for the development of simple screening methods for the detection of amyloid fibrils.

To evaluate if PTAA can be used as an optical probe for the detection of the formation of amyloid fibrils of BI, kinetic experiments following the formation of amyloids fibrils in BI were monitored by PTAA absorption. The time plot and the absorption maximum for the different solutions are shown in Figure 4a and Table S1 (Supporting Information). By plotting the ratio of the absorption intensity at 434 and 463 nm (434/463 nm), an initial lag phase, an exponential growth phase, and a final plateau phase are visible. These phases are associated with nucleation, extension, and equilibrium phases of the amyloid fibril formation process (*27*). The exponential growth phase occurs approximately during hours 4−7. The absorption maximum for PTAA is not affected until the beginning of this exponential growth phase, and during the growth phase the absorption maximum is more and more red shifted until the plateau phase is reached. The absorption spectra were also recorded for samples incubated for 24 and 72 h (data not shown), and the ratios

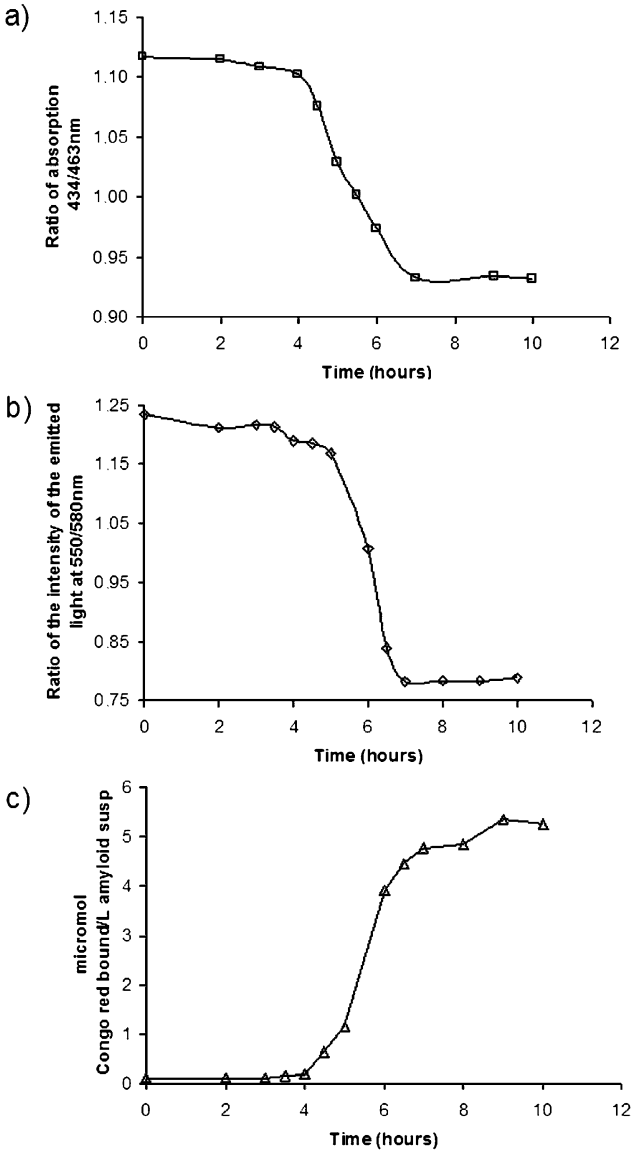

FIGURE 4: Kinetics of amyloid fibril formation of 320 μM BI, monitored by (a) PTAA absorption, (b) PTAA fluorescence, and (c) Congo red absorption. The fibrillation occurred at pH 1.6 and at 65 °C. An aliquot was withdrawn, and, after addition of the dye, the samples were diluted with 20 mM Na-phosphate to pH 7.0 (23 °C) prior to the absorption and emission measurements.

of the intensity of the emitted light at 434 and 463 nm only decreased slightly (0.93 and 0.92, respectively), as compared to the sample incubated for 10 h, indicating that the plateau phase for the amyloid fibril formation is reached after 10 h. The absorption maxima, for the samples incubated for longer time periods, were also 463 nm.

Fluorescence Measurements of BI and PTAA. The conformational changes of the polyelectrolyte chains, induced by binding to amyloid fibrils of the BI, will also alter the emission spectra of the polyelectrolyte solutions (Figure 5). After 5 min incubation in a buffer solution (20 mM Na-phosphate pH 7.0), an emission maximum of 556 nm is seen (Figure 5). Upon addition of 5 μM of nBI, the emission maximum is blue shifted to 550 nm and the intensity of the emission has increased, suggesting that the polyelectrolyte backbone becomes more nonplanar and that separation of polyelectrolyte chains occurs. Upon addition of 5 μM fBI, the emission maximum is red shifted to 577 nm (Figure 5).

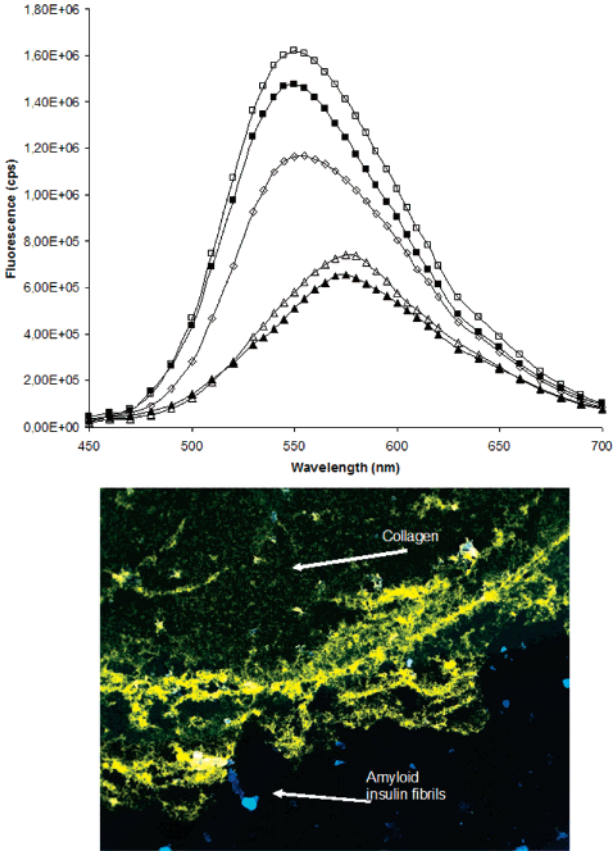

FIGURE 5: Emission spectra of 80 μM PTAA-Li (on a monomer basis) in 20 mM Na-phosphate pH 7.0 (◇), 20 mM Na-phosphate pH 7.0 with 5.0 μM nBI (□), 20 mM Na-phosphate pH 7.0 with 5.0 μM fBI (△), 20 mM Na-phosphate pH 7.0 with 5.0 μM native lysozyme (■), and 20 mM Na-phosphate pH 7.0 with 5.0 μM fibrillar form of lysozyme (▲). The emission spectra were recorded with excitation at 400 nm. Fluorescence image (bottom) of a mixture of collagen and fBI stained with PTAA. The image was recorded with an epifluorescence microscope (Zeiss Axiovert inverted microscope A200 Mot) equipped with a CCD camera (Axiocam HR), using a 405/30 nm filter (LP450, exposure time: 1500 ms).

The formation of amyloid fibrils will also decrease the intensity of the emitted light from the polyelectrolyte chains. These optical changes are associated with a planarization of the polyelectrolyte backbone and aggregation of polyelectrolyte chains (*33*−*35*), showing that the formation of β-sheet-rich amyloid fibrils of BI is influencing the conformation, the packing, and thereby the electronic structure and optical emission of the bound polyelectrolyte backbone (see Supporting Information). The geometric alteration of the polyelectrolyte chains is likely the result of different interactions of PTAA with the α-helical (nBI) and the assembled β-sheet form (fBI) of the protein. The results of the emission experiments are in good agreement with the results from the absorption measurements.

A kinetic study of the formation of amyloid fibrils in BI, using PTAA emission, was also performed. The time plot for the formation of amyloid fibrils in BI is shown in Figure 4b. The ratio of the intensity of the emitted light at 550 and 580 nm (550/580 nm) clearly indicates that the formation of amyloid fibrils is reflected as geometrical alterations of the polyelectrolyte chains. There is an initial lag phase, an exponential growth phase, and a final plateau phase represented in the plot. The exponential growth phase for amyloid fibril formation occurs during 4−7 h, in good agreement with the results obtained from the absorption measurements. The emission maximum (Table S1, Supporting Information) is not altered during the lag phase or the plateau phase, but becomes more and more red shifted during the exponential growth phase, indicating that the planarization of the polyelectrolyte backbone is due to PTAA binding to formed amyloid fibrils. On the other hand, the intensity of the emitted light is starting to decrease during the exponential growth phase and is also decreasing during the plateau phase, suggesting that the formation of longer amyloid fibrils will force the polyelectrolyte chains to aggregate. To evaluate if the intensity of the emitted light from PTAA is related to the morphology of the amyloid fibrils, further evaluation with samples incubated for longer time periods and with different protein concentrations has to be performed.

Fluorescence Measurements of Chicken Lysozyme and PTAA. To further evaluate if PTAA can be used as a conformation-sensitive optical probe for the detection of a variety of amyloid fibrils in proteins, experiments with another protein, chicken lysozyme (CL), were performed. Upon addition of 5 μM of native chicken lysozyme (nCL) to the PTAA solution, a spectrum similar to that obtained with nBI is seen (Figure 5). Likewise, after addition of 5 μM amyloid fibrillar form of lysozyme (fCL), the emission spectrum resembles the spectrum seen for the fibrillar form of BI (Figure 5). These equivalent results obtained with two completely different proteins, BI and CL, clearly indicate that PTAA is a conformation-sensitive probe and that the conformational changes of the polyelectrolyte backbone are due to a change of the protein secondary and quaternary structure that is associated with the formation of amyloid fibrils. As mentioned above, the conformational changes of the polyelectrolyte backbone are likely the result of differential interactions of PTAA with the native forms of the proteins and their non-native β-rich fibrillar counterparts. Interestingly, the change in color for two different solutions of PTAA and the different forms of lysozyme is similar to the PTAA/nBI solution and the PTAA/fBI solution, shown in Figure 3, signifying that PTAA can be useful in simple screening methods for the detection of amyloid fibrils.

Congo Red Binding Measurements. To evaluate the validity of the methodology described herein, kinetic experiments with an established probe, Congo red (*28*, *30*, *31*), were performed. The formation of amyloid fibrils in BI was followed over time with Congo red, and the time plot is shown in Figure 4c. Interestingly, the lag phase, the plateau phase, and the exponential growth phase of the formation of amyloid fibrils, approximately during 4−7 h, are almost identical to the result obtained from the absorption and emission measurements with PTAA. Hence, the results obtained with the method described in this Article are in good agreement with an established technique.

DISCUSSION

PTTA is an example of a conjugated polyelectrolyte that detects the amyloid fibril formation in vitro of two amyloidogenic proteins, insulin and lysozyme. The most widely used existing method for detection of amyloid, whether of fibrils formed in vitro from pure proteins or deposits formed in vivo in tissue sections, is staining with Congo red dye and subsequent demonstration of green-red birefringence in

cross polarized light. Interestingly, the amyloid fibril PTAA complexes prepared here exhibited both blue-green birefringence and polarized luminescence. Staining with Congo red is used principally for diagnostic purposes, and although simple to perform the procedure has many pitfalls and must be well controlled. Rapid, simple in vitro tests for detection of amyloid fibril formation are essential for a number of purposes including scientific studies of the amyloid fibril formation process, high throughput screening of amyloid fibril inhibitors, and for quality control of protein pharmaceuticals. An earlier study (*36*) of Congo red has shown that the dye binds to a variety of protein conformers including native, partially folded conformation and amyloid fibrils of several proteins and must therefore be used with caution as a diagnostic test for the presence of amyloid fibrils in vitro. Congo red was also found to induce oligomerization of native proteins (*36*). Hence, it is of great interest to find novel optical probes for the detection of the formation of amyloid fibrils. In this regard, we have shown that conformational sensitive conjugated polyelectrolytes can be used as novel optical tools for the detection of the formation of amyloid fibrils. The technique has so far been demonstrated for amyloid fibril formation in vitro, but initial experiments have shown that PTAA can be used as an amyloid specific probe in histological staining of tissue samples (work in progress).

The conjugated polyelectrolyte described in this Article binds to the native form of proteins and to the amyloid fibrillar form of proteins. These forms can easily be distinguished, due to the conformational changes of the polyelectrolyte backbone upon binding to different forms of the proteins, as minor perturbations of the geometry of the polyelectrolyte backbone are reflected as alterations of the electronic structure of the conjugated backbone. Thus, binding of the polyelectrolyte to different forms of proteins will give rise to different optical features for the conjugated polyelectrolyte. This is an improvement as compared to the small dyes used today, as these probes only change in optical feature whether they are free in solution or binding to pockets in the protein or to protein surfaces. So far, we have shown that a conjugated polyelectrolyte can be used to distinguish between the native form of proteins and the amyloid fibrillar form of proteins. Further studies are required to demonstrate whether the use of flexible conjugated polyelectrolytes instead of more rigid small molecular dyes might offer a novel approach to discriminate between pre-fibrillar aggregates, amyloid protofilaments, and amyloid fibrils. In comparison to the PTAA fluorescence signal bound to amyloid fibrils (fBI or fCL), binding of PTAA to fibers of collagen showed a spectrum similar to that of nBI (data not shown), likely due to the intrinsic polyproline type II helical structure of collagen. A mixture of collagen and fBI was also stained by PTAA, and the fluorescence image (Figure 5) clearly shows distinct changes in color from PTAA, depending on which protein the conjugated polyelectrolyte is bound to. The difference in color of the fBI fibers in this picture as compared to the fibers seen in Figure 2 is due to the fact that the images were taken using different filters (see Experimental Procedures) and that the fibers were stained with PTAA at different pH values.

CPs-based sensors are also sensitive to minor perturbations, due to amplification by a collective system response, and offer a key advantage as compared to small molecule elements (*37*, *38*). Other merits of this method as compared to the use of small molecule dyes are that the shift in absorption, due to the conformational alteration of the polyelectrolyte backbone, is clearly visible for the human eye and that the formation of the amyloid fibrils in vitro can be followed by both absorption and emission. Furthermore, Congo red aggregates and precipitates within minutes upon interactions with large clusters of insulin fibrils, which complicates absorption measurements. No precipitation was observed in solutions of insulin fibrils and PTAA.

In conclusion, we have shown that a negatively charged conjugated polyelectrolyte can be used as a novel optical probe for the detection of the formation of amyloid fibrils. The formation of amyloid fibrils is reflected as an alteration of the geometry and the electronic structure of the bound polyelectrolyte chains and has so far been detected by absorption and emission, but electrical detection of these transitions will most likely be possible. The method is fast and simple and is based on noncovalent assembly between the anionic polyelectrolyte and the protein. As formation of amyloid fibrils in vivo can lead to disease and complicate biotechnological purification of proteins in vitro, a simple detection tool of such a process is of great importance. We suggest that the method described in this Article may be used for a wide range of proteins, biosensors, and bioelectronic devices.

ACKNOWLEDGMENT

We thank Mats R. Andersson and co-workers, Chalmers University, Sweden, for the synthesis of PTAA.

SUPPORTING INFORMATION AVAILABLE

CD measurements of BI, fluorescence measurements of BI and PTAA, a table of absorption and emission maxima for PTAA mixed with BI, and time plots of absorption and emission maxima PTAA mixed with BI. This material is available free of charge via the Internet at http://pubs.acs.org.

REFERENCES

1. Wang, J., Wang, D., Miller, E. K., Moses, D., Bazan, G. C., and Heeger, A. J. (2000) Photoluminescence of water-soluble conjugated polymers: origin of enhanced quenching by charge transfer, *Macromolecules 33*, 5153−5158.
2. Fan, C., Plaxco, K. W., and Heeger, A. J. (2002) High-efficiency fluorescence quenching of conjugated polymers by proteins, *J. Am. Chem. Soc. 124*, 5642−5643.
3. Wang, D., Gong, X., Heeger, P. S., Rininsland, F., Bazan, G. C., and Heeger, A. J. (2002) Biosensors from conjugated polyelectrolyte complexes, *Proc. Natl. Acad. Sci. U.S.A. 99*, 49−53.
4. Gaylord, B. S., Heeger, A. J., and Bazan, G. C. (2002) DNA detection using water-soluble conjugated polymers and peptide nucleic acid probes, *Proc. Natl. Acad. Sci. U.S.A. 99*, 10954−10957.
5. Gaylord, B. S., Heeger, A. J., and Bazan, G. C. (2003) DNA hybridization detection with water-soluble conjugated polymers and chromophore-labeled single-stranded DNA, *J. Am. Chem. Soc. 125*, 896−900.
6. Liu, B., Gaylord, B. S., Wang, S., and Bazan, G. C. (2003) Effect of chromophore-charge distance on the energy transfer properties of water-soluble conjugated oligomers, *J. Am. Chem. Soc. 125*, 6705−6714.
7. Ho, H.-A., Boissinot, M., Bergeron, M. G., Corbeil, G., Dore, K., Boudreau, D., and Leclerc, M. (2002) Colorimetric and fluorometric detection of nucleic acids using cationic polythiophene derivatives, *Angew. Chem., Int. Ed. 41*, 1548−1551.

8. Nilsson, K. P. R., and Inganäs, O. (2003) Chip and solution detection of DNA hybridisation using a luminescent zwitter-ionic polythiophene derivative, *Nat. Mater. 2*, 419−424.
9. Ho, H.-A., and Leclerc, M. (2004) Optical sensors based on hybrid aptamer/conjugated polymer complexes, *J. Am. Chem. Soc. 126*, 1384−1387.
10. Nilsson, K. P. R., Rydberg, J., Baltzer, L., and Inganäs, O. (2003) Self-assembly of synthetic peptides control conformation and optical properties of a zwitterionic polythiophene derivative, *Proc. Natl. Acad. Sci. U.S.A. 100*, 10170−10174.
11. Nilsson, K. P. R., Rydberg, J., Baltzer, L., and Inganäs, O. (2004) Twisting macromolecular chains − self-assembly of a chiral supermolecule from nonchiral polythiophene polyanions and random coil synthetic peptides, *Proc. Natl. Acad. Sci. U.S.A. 101*, 11197−11202.
12. Nilsson, K. P. R., and Inganäs, O. (2004) Optical emission of a conjugated polyelectrolyte: Calcium-induced conformational changes in calmodulin and calmodulin-calcineurin interactions, *Macromolecules 37*, 9109−9113.
13. Carrell, R. W., and Lomas, D. A. (1997) Conformational disease, *Lancet 350*, 134−138.
14. Terzi, E., Hölzemann, G., and Seelig, J. (1997) Interaction of Alzheimer beta-amyloid peptide(1−40) with lipid membranes, *Biochemistry 36*, 14845−14852.
15. Matsuzaki, K., and Horikiri, C. (1999) Interactions of amyloid beta-peptide (1−40) with ganglioside-containing membranes, *Biochemistry 38*, 4137−4142.
16. Kelly, J. W. (2002) Towards an understanding of amyloidogenesis, *Nat. Struct. Biol. 9*, 323−325.
17. Sunde, M., Serpell, L. C., Bartlam, M., Fraser, P. E., Pepys, M. B., and Blake, C. C. (1997) Common core structure of amyloid fibrils by synchrotron X-ray diffraction, *J. Mol. Biol. 273*, 729−739.
18. Dobson, C. M. (1999) Protein misfolding, evolution and disease, *Trends Biochem. Sci. 24*, 329−332.
19. Hammarström, P., Jiang, X., Hurshman, A. R., Powers, E. T., and Kelly, J. W. (2002) Sequence-dependent denaturation energetics: A major determinant in amyloid disease diversity, *Proc. Natl. Acad. Sci. U.S.A. 99*, 16427−16432.
20. Blundell, T. L., Cutfield, J. F., Dodson, G. G., Dodson, E., Hodgkin, D. C., and Mercola, D. (1971) Atomic positions in rhombohedral 2-zinc insulin crystals, *Nature (London) 231*, 506−511.
21. Gursky, O., Badger, J., Li, Y., and Caspar, D. L. (1992) Conformational changes in cubic insulin crystals in the pH range 7−11, *Biophys. J. 63*, 1210−1220.
22. Waugh, D. F. (1946) A fibrous modification of insulin. I. The heat precipitate of insulin, *J. Am. Chem. Soc. 68*, 247−250.
23. Nielsen, L., Frokjaer, S., Carpenter, J. F., and Brange, J. (2001) Studies of the structure of insulin fibrils by Fourier transform infrared (FTIR) spectroscopy and electron microscopy, *J. Pharm. Sci. 90*, 29−37.
24. Nielsen, L., Khurana, R., Coats, A., Frokjaer, S., Brange, J., Vyas, S., Uversky, V. N., and Fink, A. L. (2001) Effect of environmental factors on the kinetics of insulin fibril formation: elucidation of the molecular mechanism, *Biochemistry 40*, 6036−6046.
25. Nettleton, E. J., Tito, P., Sunde, M., Bouchard, M., Dobson, C. M., and Robinson, C. V. (2000) Characterization of the oligomeric states of insulin in self-assembly and amyloid fibril formation by mass spectrometry, *Biophys. J. 79*, 1053−1065.
26. Bouchard, M., Zurdo, J., Nettleton, E. J., Dobson, C. M., and Robinson, C. V. (2000) Formation of insulin amyloid fibrils followed by FTIR simultaneously with CD and electron microscopy, *Protein Sci. 9*, 1960−1967.
27. Ahmad, A., Millett, I. S., Doniach, S., Uversky, V. N., and Fink, A. L. (2003) Partially folded intermediates in insulin fibrillation, *Biochemistry 42*, 11404−11416.
28. Glenner, G. G. (1981) The bases of the staining of amyloid fibers: their physicochemical nature and the mechanism of their dye-substrate interaction, *Prog. Histochem. Cytochem. 13*, 1−37.
29. Ding, L., Jonforsen, M., Roman, L. S., Andersson, M. R., and Inganas, O. (2000) Photovoltaic cells with a conjugated polyelectrolyte, *Synth. Met. 110*, 133−140.
30. Klunk, W. E., Pettegrew, J. W., and Abraham, D. J. (1989) Quantitative evaluation of congo red binding to amyloid-like proteins with a beta-pleated sheet conformation, *J. Histochem. Cytochem. 37*, 1273−1281.
31. Klunk, W. E., Pettegrew, J. W., and Abraham, D. J. (1989) Two simple methods for quantifying low-affinity dye-substrate binding, *J. Histochem. Cytochem. 37*, 1293−1297.
32. Kim, B., Chen, L., Gong, J., and Osada, Y. (1999) Titration behavior and spectral transitions of water-soluble polythiophene carboxylic acids, *Macromolecules 32*, 3964−3969.
33. Langeveld-Voss, B. M. W., Janssen, R. A. J., Christiaans, M. P. T., Meskers, S. C. J., Dekkers, H. P. J. M., and Meijer, E. W. (1996) Circular dichroism and circular polarization of photoluminescence of highly ordered poly{3,4-di (*S*)-2-methylbutoxy thiophene}, *J. Am. Chem. Soc. 118*, 4908−4909.
34. Langeveld-Voss, B. M. W., Janssen, R. A. J., and Meijer, E. W. (2000) On the origin of optical activity in polythiophenes, *J Mol. Struct. 521*, 285−301.
35. Nilsson, K. P. R., Andersson, M. R., and Inganäs, O. (2002) Conformational transitions of a free amino acid-functionalized polythiophene induced by different buffer systems, *J. Phys.: Condens. Matter 14*, 10011−10020.
36. Khurana, R., Uversky, V. N., Nilesen, L., and Fink, A. L. (2001) Is Congo red an amyloid-specific dye, *J. Biol. Chem. 276*, 22715−22721.
37. Zhou, Q., and Swager, T. M. (1995) Method for enhancing the sensitivity of fluorescent chemosensors: energy migration in conjugated polymers, *J. Am. Chem. Soc. 117*, 7017−7018.
38. Chen, L., McBranch, D. W., Wang, H.-L., Helgeson, R., Wudl, F., and Whitten, D. G. (1999) Highly sensitive biological and chemical sensors based on reversible fluorescence quenching in a conjugated polymer, *Proc. Natl. Acad. Sci. U.S.A. 96*, 12287−12292.

BI047402U